Thermochimica Acta, 129 (1988) 77–87
Elsevier Science Publishers B.V., Amsterdam – Printed in The Netherlands

A THERMODYNAMIC EVALUATION OF THE IRON–ZINC SYSTEM

STEPHAN PETERSEN, PHILIP J. SPENCER and KLAUS HACK

Lehrstuhl für Theoretische Hüttenkunde und Metallurgie der Kernbrennstoffe der RWTH Aachen, Kopernikusstrasse 16, D-5100 Aachen (F.R.G.)

(Received 21 January 1988)

ABSTRACT

Experimental thermodynamic properties and phase equilibrium data have been used in deriving a thermodynamically consistent analytical description of the thermochemical properties and phase diagram of the Fe–Zn system. A set of coefficients is used to describe the conventional Gibbs free energy of the pure components and stoichiometric intermetallic compounds and the excess Gibbs energies of the solution phases are given. Thermodynamic and phase boundary values calculated with these coefficients agree well with experimental data within experimental error.

INTRODUCTION

Since galvanizing is a surface refinement of major technological importance for iron and steel products, many investigations of phase equilibria in the Fe–Zn system have been made. Differences in the published phase diagrams have made it clear that uncertainties still exist concerning the phase boundaries of the solution phases as well as the number of intermetallic compound phases and their properties. On the other hand, thermodynamic data for the Fe–Zn system are of special interest for high temperature process metallurgy, since the presence of zinc, even in small amounts, causes problems in the blast furnace and in recycling operations, mainly due to its low melting point and high vapour pressure even at relatively low temperatures.

METHOD OF CALCULATION

To represent the conventional Gibbs free energy functions for the pure substances and stoichiometric intermetallic compounds, an equation of the form

$$G = a + bT + cT \ln T + dT^2 + eT^3 + f(1/T) \quad (1)$$

Dedicated to Professor Oswald Kubaschewski in honour of his contribution to thermochemistry.

0040-6031/88/$03.50

has been used. With the resulting table of coefficients a, b, c,... and the thermodynamic relations

$$S = -(\partial G/\partial T)_p, \qquad H = G + TS \tag{2}$$

it is possible to calculate for example

$$H(T) = a - cT - dT^2 - 2eT^3 + 2f(1/T) \tag{3}$$

or

$$S(T) = -(b + c) - 2dT - c \ln T - 3eT^2 + f(1/T^2) \tag{4}$$

The analytical description of the thermodynamic properties of a binary system's solution phases can be realized in many cases with the equation for the formation of substitutional solid solution series

$$G_m = \sum_{i=1}^{2} x_i G_i(T) + \Delta G^{id}(T, x) + \Delta G^{E}(T, x) \tag{5}$$

where $\Delta G^{id} = -T\Delta S^{id} = RT(x_1 \ln x_1 + x_2 \ln x_2)$. The term $x_i G_i(T)$ represents the contribution of the pure component i to the molar Gibbs energy of the solution phase, ΔG^{id} indicates the ideal part of the molar Gibbs energy of mixing. The excess part ΔG^{E} of the molar Gibbs energy of mixing is described by a Redlich–Kister equation of the form

$$\Delta G^{E} = x_i x_j \sum_{\nu=0}^{n} (x_i - x_j)^{\nu} L_{ij}^{(\nu)}(T) \tag{6}$$

where $L_{ij}^{(\nu)}(T) = A_{ij}^{(\nu)} + B_{ij}^{(\nu)} T$ (i = Fe, j = Zn). The coefficients are linear functions of temperature, i.e. $A_{ij}^{(\nu)}$ and $B_{ij}^{(\nu)}$ correspond to the temperature-independent values of the enthalpy and excess entropy of mixing. $G(T)$ functions for the pure components can usually be taken from literature, while the polynomial expressions for $G(T)$ of the stoichiometric intermetallic compounds and for the excess Gibbs energy ΔG^{E} as a function of temperature and composition for the solution phases must be generated. This is done by a computer program written by Lukas et al. [1] which calculates the optimized $G(T)$ polynomial expressions for the stoichiometric intermetallic compounds and the ΔG^{E} coefficients of the solution phases by means of a least-squares method, using experimental thermodynamic and phase boundary values as input data.

The temperature dependence of the Gibbs energy for the solution phases is also described by eqn. (1), while the Redlich–Kister equation describes the concentration dependence of the excess Gibbs energy.

APPLICATION OF THE MODEL EQUATION TO THE IRON–ZINC SYSTEM

The Gibbs energies of the pure elements in the different stable and metastable phase states are listed in Table 1. Because of their rather narrow

TABLE 1

Conventional Gibbs energies for the Fe–Zn system (including the intermetallic phases). $G = a + bT + cT \ln T + dT^2 + eT^3 + f(1/T)$ (J g-atom^{-1})

	a	b	c	d	e	f
Liquid phase						
Fe298–2500 K	−10321.1	290.975	−46.0240	0	0	0
Zn298–2000 K	−3629.07	161.624	−31.38	0	0	0
fcc phase						
Fe(fcc)	−234.73	132.389	−24.6643	-3.75752×10^{-3}	-5.89269×10^{-8}	77358.5
Zn(fcc)	−4178.2	98.8181	−20.7359	-6.2551×10^{-3}	0	−41631
bcc phase						
Fe						
298–800 K	−9267.47	161.985	−28.1751	3.65891×10^{-3}	-4.17354×10^{-6}	144766
800–1000 K	221875	−1925.19	263.454	-1.27905×10^{-1}	0	-3.09616×10^{-7}
1000–1042 K	318138	−4446.39	641.905	-3.48169×10^{-1}	0	0
1042–1060 K	−1030290	13538.5	−1946.25	8.93748×10^{-1}	0	0
1060–1180 K	711174	−4322.46	−56.1932	-1.67071×10^{-1}	0	-1.45606×10^{8}
1180–1666 K	−4523.79	136.634	−23.9911	-9.47472×10^{-3}	9.22150×10^{-7}	0
1666–1809 K	−1640.83	134.708	−24.6354	-4.95176×10^{-3}	0	0
Zn						
298–1811 K	−3572.2	98.0015	−20.7359	-6.2551×10^{-3}	0	−41631
Zn(hcp) phase						
Zn(hcp)	−6459.2	100.5115	−20.7359	-6.2551×10^{-3}	0	−41631
Γ phase						
Fe(bcc) [a]	1224.83	124.134	−23.5143	-4.39752×10^{-3}	-5.89269×10^{-8}	77358.5
Zn(bcc)	−3572.2	98.0015	−20.7359	-6.2551×10^{-3}	0	−41631
Intermetallic phases						
Γ_1 ($FeZn_4$)	−10287.0	106.4423	−21.2916	-5.88357×10^{-3}	-1.17854×10^{-8}	−17832.9
δ ($FeZn_7$)	−11887.3	106.3016	−21.0832	-6.02289×10^{-3}	-7.36586×10^{-9}	−26757.1
ζ ($FeZn_{13}$)	−9430.5	103.0370	−20.9343	-6.12245×10^{-3}	-4.20738×10^{-9}	−33135.0

[a] Non-magnetic bcc iron.

solubility range and the lack of low-temperature experimental data, the Γ_1-, δ-, and ζ-phases are treated as stoichiometric intermetallic compounds. In the same manner as for the component elements, the stoichiometric intermetallic compounds are each represented by one $G(T)$ function. The coefficients of these functions were derived by applying Neumann-Kopp's rule for the specific heat to the data of the pure components. The values for standard enthalpy and entropy of these line compounds, which are described by the coefficients a and b of eqn. (1), are also optimized by the assessment program in order to represent the experimental data as consistently as possible. The resulting coefficients of the $G(T)$ functions are also listed in Table 1, while calculated values of ΔH_{298} and S_{298} are given in Table 6.

The data describing the Gibbs free energies of pure Fe in its stable structures (bcc, fcc and liquid) were taken from data proposed by Dinsdale [2]. Lattice stability values for Fe in the Γ structure, which according to Villars and Calvert [3] is bcc-type, were obtained from data for non-magnetic Fe(bcc) given by Guillermet and Gustafson [4], while the $G(T)$ function for Zn(bcc) was derived by combining data for the transformation energy Zn(hcp $\rightarrow$ bcc) given by Kaufman and Bernstein [5] with the $G(T)$ function for Zn(hcp) from the Barin et al. tables [6]. These data for non-magnetic Fe(bcc) and Zn(bcc) were also used to calculate the C_p functions of the Γ_1-, δ-, and ζ-phases. The data for Zn(fcc) needed to calculate the γ-loop were taken from Murray [7].

Before improved descriptions of the entire Fe–Zn system could be obtained by optimizing data for all the phases together, optimized coefficients representing experimental and phase boundary data were obtained for each phase of the system in succession. Table 2 shows the coefficients of excess

TABLE 2

Excess Gibbs energy ΔG^E coefficients for the liquid, bcc, fcc, and Γ phases of the Fe–Zn system. $\Delta G^E = x_i x_j \sum_{\nu=0}^{n} (x_i - x_j)^\nu L_{ij}^{(\nu)}(T)$ (J g-atom^{-1}) where $L_{ij}^{(\nu)}(T) = A_{ij}^{(\nu)} + B_{ij}^{(\nu)} T$ (i = Fe, j = Zn)

Phase	ν	$A_{FeZn}^{(\nu)}$	$B_{FeZn}^{(\nu)}$
Liquid	0	89265.3	−57.3528
	1	−87202.6	70.3784
	2	−86630.9	42.7867
fcc	0	20266.6	−10.5944
	1	11609.8	−8.3663
	2	−21375.4	17.8193
bcc	0	14135.9	−5.4381
	1	30711.7	−27.5599
	2	−38550.0	34.6443
Γ	0	−23255.2	33.2288
	1	12488.1	9.0758
	2	−27457.7	27.3051

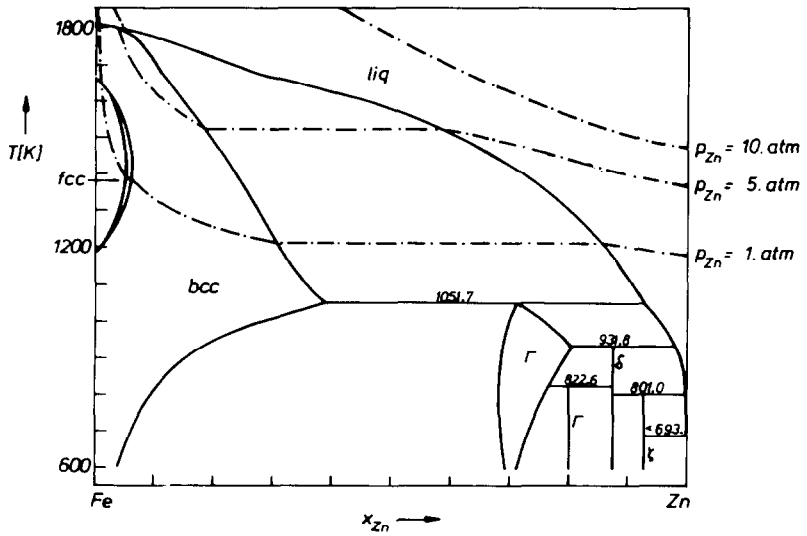

Fig. 1. Calculated phase diagram for the Fe–Zn system using evaluated data.

Gibbs free energy of mixing as the result of the optimization procedure, while Fig. 1 presents the calculated phase diagram.

EXPERIMENTAL PHASE DIAGRAM INFORMATION

The Fe–Zn phase diagram has been the subject of much controversy since the earliest investigations of the system, in particular with regard to the phases forming at high zinc concentrations, their ranges of temperature and stoichiometry in which they are stable. The results of three separate investigations published in 1936 [8–10] already show discrepancies of the order of 20–30 K in observed peritectic temperatures as well as in the number of phases forming in Zn-rich alloys.

Schramm [10–12] carried out a series of investigations of the system and presented a phase diagram in the final publication. In 1970 Bühler et al. [13] reported the existence of two separate δ-phases instead of the single δ-phase found in earlier investigations. The two phases were confirmed by Ghoniem [14] and Ghoniem and Löhberg [15] in 1972. Kirchner et al. [16] re-investigated Fe-rich alloys and found a closed γ-loop without a minimum, contrary to the observation of previous authors.

Finally the existence of a Γ_1-phase was proposed by Bastin et al. [17] in 1974, with a solubility range of 18.5 to 23.5 atm.% Fe and a peritectic temperature close to 550 °C. In 1977 Bastin et al. [18] negated the existence of two separate δ_{ip} and δ_{ik} phases as well as the existence of a high-temperature δ-phase. In 1979 and 1980 Gellings and coworkers [19,20] carried out

further research work on the phase diagram and on the δ- and ζ-phases in particular. Kubaschewski's [21] evaluated Fe–Zn phase diagram is constituted mainly from the phase diagram data given by Bastin and coworkers, combined with Gellings' results. Since Kubaschewski took all data published for the Fe–Zn phase diagram into consideration and her evaluation appears to be very consistent, it has been used as the primary source of phase diagram data for the present calculations.

EXPERIMENTAL THERMOCHEMICAL DATA

Most experimental investigations of the Fe–Zn system have been concerned with phase diagram determinations and only few papers containing thermodynamic data are available. Wriedt [22] measured zinc vapour pressures of bcc solutions at 757, 793, and 900 °C. According to his work, both Zn and Fe show large, positive, and moderately temperature-sensitive deviations from ideality; excess enthalpies and Gibbs energies are positive in the ranges studied.

Positive deviations from ideality were also found by Tomita et al. [23] using a transportation method to study alloys over the entire composition range for temperatures between 973 and 1073 K. Their activity data agree well with Wriedt's values, being slightly higher for the Fe-rich samples.

By e.m.f. measurement with a $Zn/(KCl + LiCl) + ZnCl_2/Zn_xFe_{1-x}$ cell, Abu Ali et al. [24]) obtained Gibbs energies for Fe-Zn alloys containing 2.2 to 80% Zn, calculated for 900 K. Gellings et al. [25] used the Knudsen effusion method to investigate the thermodynamic properties of the system. Vapour pressures, activities, and integral Gibbs free energies were calculated for the different phases at 617 K.

Some enthalpy and entropy values were taken from Reutner and Engell's results [26], from experiments on the electrochemical deposition of zinc on iron from a salt bath at temperatures between 370 and 570 °C. However, they had to be omitted during the optimizing calculations due to their very large mean-square error.

Dimov et al. [27] determined activities of Zn in Fe-rich liquid alloys for a temperature of 1585 °C and mole fractions to $x_{Zn} = 0.005$ using a vapour pressure method. Their activities also exhibit a positive deviation from ideality. The experimental values had to be read from a small plot in their publication and are therefore less certain. Pluschkell [28] recently investigated Fe-rich liquid alloys containing up to 2 mass% Zn at 1600 °C.

DISCUSSION

Using the set of coefficients obtained from the optimization process (Table 2), the phase diagram shown in Fig. 1 has been calculated. There is

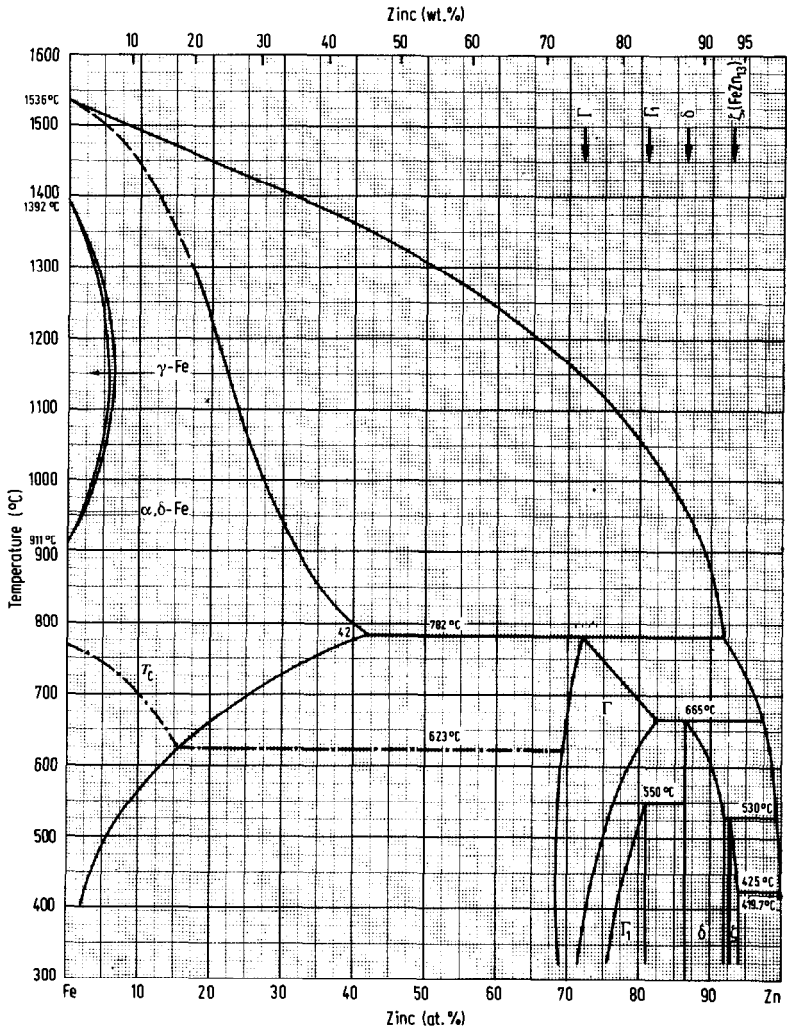

Fig. 2. Fe–Zn phase diagram according to Kubaschewski [21].

excellent agreement with the diagram presented by Kubaschewski (Fig. 2), as is evidenced by the comparison of 2- and 3-phase equilibrium information for the system presented in Table 3. The only tendency to discrepancy with the experimental diagram is at low temperatures in Fe-rich alloys, where the higher Zn solubility given by the calculations may be due to the fact that the ferromagnetism of Fe–Zn alloys in this composition range has not been explicitly described in the present calculation.

Although the Γ_1-, δ-, and ζ-phases have been treated here as "line compounds", this simplification does not result in significant differences between the calculated and experimental peritectic temperatures of formation of the compounds.

TABLE 3

Experimental and calculated 2- and 3-phase-equilibria of the Fe–Zn system

Equilibrium	Experimental results	Calculated results
Peritectic	$T = 1055$ K, $x_{Zn}^{bcc} = 0.42$	$T = 1051.68$K, $x_{Zn}^{bcc} = 0.389$
bcc + liq → Γ	$x_{Zn}^{\Gamma} = 0.72$	$x_{Zn}^{\Gamma} = 0.712$
	$x_{Zn}^{liq} = 0.92$	$x_{Zn}^{liq} = 0.928$
Peritectic	$T = 938$ K, $x_{Zn}^{\Gamma} = 0.825$	$T = 931.83$K, $x_{Zn}^{\Gamma} = 0.806$
Γ + liq → δ	$x_{Zn}^{\delta} = 0.865$	$x_{Zn}^{\delta} = 0.875$
	$x_{Zn}^{liq} = 0.975$	$x_{Zn}^{liq} = 0.980$
Peritectic	$T = 823$ K, $x_{Zn}^{\Gamma} = 0.765$	$T = 822.61$K, $x_{Zn}^{\Gamma} = 0.767$
Γ + δ → Γ_1	$x_{Zn}^{\Gamma_1} = 0.81$	$x_{Zn}^{\Gamma_1} = 0.80$
	$x_{Zn}^{\delta} = 0.865$	$x_{Zn}^{\delta} = 0.875$
Peritectic	$T = 803$ K, $x_{Zn}^{\delta} = 0.92$	$T = 800.95$K, $x_{Zn}^{\delta} = 0.875$
δ + liq → ζ	$x_{Zn}^{\zeta} = 0.927$	$x_{Zn}^{\zeta} = 0.929$
	$x_{Zn}^{liq} = 0.995$	$x_{Zn}^{liq} = 0.999$
bcc + liq	$T = 1573$ K, $x_{Zn}^{bcc} = 0.173$	$T = 1573$ K, $x_{Zn}^{bcc} = 0.162$
	$x_{Zn}^{liq} = 0.520$	$x_{Zn}^{liq} = 0.512$
	$T = 1373$ K, $x_{Zn}^{bcc} = 0.237$	$T = 1373$ K, $x_{Zn}^{bcc} = 0.249$
	$x_{Zn}^{liq} = 0.765$	$x_{Zn}^{liq} = 0.747$
	$T = 1173$ K, $x_{Zn}^{bcc} = 0.321$	$T = 1173$ K, $x_{Zn}^{bcc} = 0.323$
	$x_{Zn}^{liq} = 0.891$	$x_{Zn}^{liq} = 0.877$
bcc + Γ	$T = 973$ K, $x_{Zn}^{bcc} = 0.254$	$T = 973$ K, $x_{Zn}^{bcc} = 0.236$
	$x_{Zn}^{\Gamma} = 0.704$	$x_{Zn}^{\Gamma} = 0.693$
	$T = 773$ K, $x_{Zn}^{bcc} = 0.056$	$T = 773$ K, $x_{Zn}^{bcc} = 0.085$
	$x_{Zn}^{\Gamma} = 0.675$	$x_{Zn}^{\Gamma} = 0.683$

The present thermodynamic evaluation of the Fe–Zn system reveals clearly the rather large discrepancies between the experimental results of different authors. This is in part because the vapour pressure of zinc reaches

TABLE 4

Two-phase-equilibria of 1-atm isobar

$T = 1807.65$ K, $x_{Zn}^{liq} = 6.64 \times 10^{-3}$
$x_{Zn}^{bcc} = 5.87 \times 10^{-3}$
$T = 1653.25$ K, $x_{Zn}^{bcc} = 1.15 \times 10^{-2}$
$x_{Zn}^{fcc} = 1.09 \times 10^{-2}$
$T = 1386.70$ K, $x_{Zn}^{fcc} = 5.26 \times 10^{-2}$
$x_{Zn}^{bcc} = 6.23 \times 10^{-2}$
$T = 1212.62$ K, $x_{Zn}^{bcc} = 3.08 \times 10^{-1}$
$x_{Zn}^{liq} = 8.56 \times 10^{-1}$

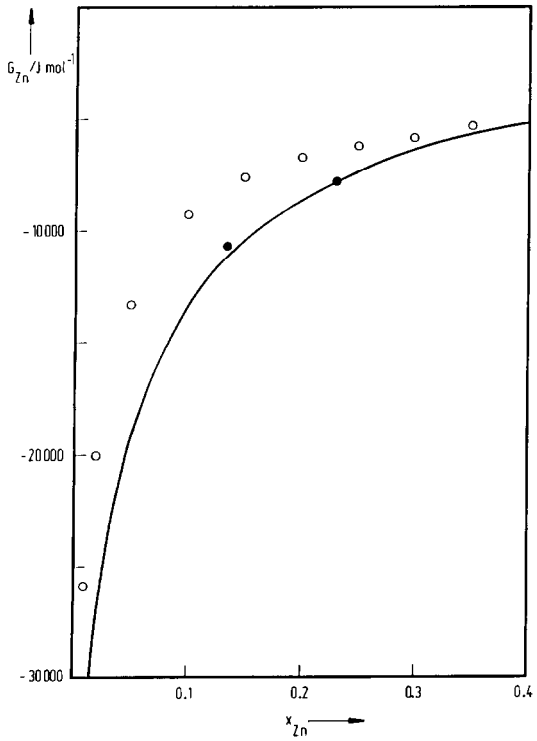

Fig. 3. Partial Gibbs energy of Zn in bcc Fe–Zn alloys at 1066 K: reference state Zn(liquid). ○ Wriedt [22]; ● Tomita at al. [23]; ——— Calculated.

1 atm below 950 °C over a very wide composition range in the system. Phase boundary determinations and thermodynamic measurements are thereby made more difficult to carry out accurately. Calculated Zn isobars for 1, 5, and 10 atm are included in Fig. 1 to demonstrate the metastable nature of

TABLE 5

A comparison of experimental Gibbs energy data at 617 K from Gellings et al. [25] with calculated values

Phase	x_{Zn}	$G^f_{meas.}$ (kJ g-atom^{-1})	$G^f_{calc.}$ (kJ g-atom^{-1})
bcc	0.082	−0.9	−0.6
Γ	0.687	−5.0	−3.6
Γ_1	0.8	−5.5	−3.9
δ	0.868	−5.4	
	0.875		−4.2
	0.900	−5.1	
ζ	0.928	−4.1	
	0.929		−2.8

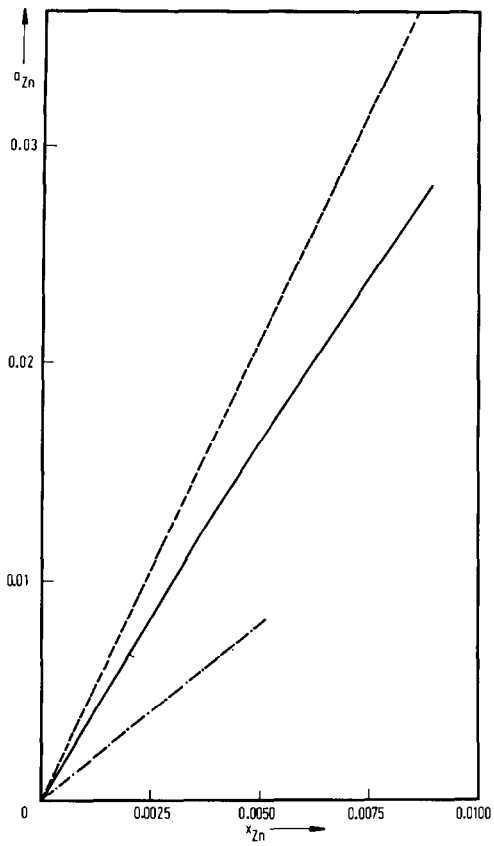

Fig. 4. Experimental and calculated activity of Zn in liquid Fe–Zn alloys at 1600 °C. — — — Pluschkell [28]; ·–·–· Dimov at al. [27]; ——— calculated.

the illustrated high-temperature phase equilibria at 1 atm total pressure and to present information of practical importance, e.g. for steel-making and galvanizing processes. The calculated 2-phase equilibria associated with the 1-atm isobar are given in Table 4. Figure 3 shows the extent of the agreement between experimental [22,23] and calculated partial Gibbs energies of Zn in the bcc phase of the system, and Fig. 4 presents calculated and experimental [27,28] activity values in Fe-rich liquid alloys. Note that

TABLE 6

Assessed ΔH_{298} and S_{298} values of the stoichiometric intermetallic compounds

Phase	ΔH_{298} (J g-atom^{-1})	S_{298} (J g-atom^{-1} K^{-1})
Γ ($FeZn_4$)	−3534.90	39.4712
δ ($FeZn_7$)	−5245.05	38.1975
ζ ($FeZn_{13}$)	−2866.74	40.4517

for this diagram the composition range is very limited (0–1 atm.% Zn). In Table 5, calculated Gibbs energies of formation for the solid phases of the system are compared with the data determined experimentally by Gellings et al. [25] at 617 K. Table 6 lists the values of ΔH_{298} and S_{298} for the Γ_1-, δ-, and ζ-phases as obtained from the present evaluation.

REFERENCES

1 H.L. Lukas, E.-Th. Henig and B. Zimmermann, Calphad, 1 (1977) 225.
2 A.T. Dinsdale, National Physical Laboratory, 1985, in preparation for publication by Scientific Group Thermodata Europe (SGTE).
3 P. Villars and L.D. Calvert, Pearson's Handbook of Crystallographic Data for Intermetallic Phases, Volume 3, Am. Soc. Met., Metals Park, Ohio, 1985.
4 A.F. Guillermet and P. Gustafson, An Assessment of the Thermodynamic Properties and $P-T$ Phase Diagram of Iron, Materials Center, Royal Inst. Technology, Stockholm, 1984.
5 L. Kaufman and H. Bernstein, Computer Calculation of Phase Diagrams, Academic Press, New York and London, 1970.
6 I. Barin, O. Knacke and O. Kubaschewski, Thermochemical Properties of Inorganic Substances, Springer-Verlag, New York, 1977.
7 J.L. Murray, Bull. Alloy Phase Diagrams, 4 (1983) 55.
8 M. Hansen, Der Aufbau der Zweistofflegierungen, Springer-Verlag, Berlin, 1936.
9 E.C. Truesdale, R.D. Wilcox and J.L. Rodda, Trans. AIME, 122 (1936) 192.
10 J. Schramm, Z. Metallkd., 28 (1936) 203
11 J. Schramm, Z. Metallkd., 29 (1937) 222.
12 J. Schramm, Z. Metallkd., 30 (1938) 122, 131; 30 (1938) 327.
13 H.E. Bühler, G. Jackel, L. Meyer and S. Baumgartl, Microchim. Acta., Suppl. IV (1970) 75.
14 M.A. Ghoniem, Beitrag zur Aufklärung der Reaktionsvorgänge zwischen flüssigem Zink und festem Eisen, Thesis, Berlin, 1972.
15 M.A. Ghoniem and K. Löhberg, Metall, 10 (1972) 1026.
16 G. Kirchner, H. Harvig, K.-R. Moquist and M. Hillert, Arch. Eisenhüttenwes., 44 (1973) 227.
17 G.F. Bastin, F.J.J. Van Loo and G.D. Rieck, Z. Metallkd., 65 (1974) 656.
18 G.F. Bastin, F.J.J. Van Loo and G.D. Rieck, Z. Metallkd., 68 (1977) 359.
19 P.J. Gellings, E.W. De Bree and G. Giermann, Z. Metallkd., 70 (1979) 312, 315.
20 P.J. Gellings, G. Giermann, D. Koster and J. Kuit, Z. Metallkd., 71 (1980) 70.
21 O. Kubaschewski, Iron—Binary Phase Diagrams, Springer-Verlag, Berlin, 1982.
22 H.A. Wriedt, Trans. AIME, 239 (1967) 1120.
23 M. Tomita, T. Azakami, L.M. Timberg and J.M. Toguri, Trans. AIME 22 (1981) 717.
24 S. Abu Ali, G.A. Vinokurova and V.A. Geiderikh, Khim. Termodin. Termokhim., (1979) 201.
25 P.J. Gellings, D. Koster, J. Kuit and T. Fransen, Z. Metallkd. 71 (1980) 150.
26 P. Reutner and H.-J. Engell, Arch. Eisenhüttenwes., 51 (1980) 457.
27 I. Dimov, D. Nenov, N. Gidikova and A. Mozeva, Arch. Eisenhüttenwes., 48 (1977) 209.
28 W. Pluschkell, private communication, 1986.